Published July 24, 2015

Bare Soil Carbon Dioxide Fluxes with Time and Depth Determined by High-Resolution Gradient-Based Measurements and Surface Chambers

X. Xiao
X. Kuang
Soil Science Dep.
North Carolina State Univ.
Raleigh, NC 27695

T.J. Sauer
USDA–ARS
National Lab. for Agriculture and Environment
Ames, IA 50011

J.L. Heitman*
Soil Science Dep.
North Carolina State Univ.
Raleigh, NC 27695

R. Horton
Agronomy Dep.
Iowa State Univ.
Ames, IA 50011

Soil CO_2 production rates and fluxes vary with time and depth. The shallow near-surface soil layer is important for myriad soil processes, yet knowledge of dynamic CO_2 concentrations and fluxes in this complex zone is limited. We used a concentration gradient method (CGM) to determine CO_2 production and effluxes with depth in shallow layers of a bare soil. The CO_2 concentration was continuously measured at 13 depths in the 0- to 200-mm soil layer. For an 11-d period, 2% of the soil CO_2 was produced below a depth of 175 mm, 8% was produced in the 50- to 175-mm soil layer, and 90% was produced in the 0- to 50-mm soil layer. Soil CO_2 concentration showed similar diurnal patterns with temperature in deeper soil layers and out-of-phase diurnal patterns in surface soil layers. Soil CO_2 flux from most of the soil layers can be described by an exponential function of soil temperature, with temperature sensitivity (Q_{10}) ranging from 1.40 to 2.00 (1.62 ± 0.17). The temperature-normalized CO_2 fluxes are related to soil water content with a positive linear relationship in surface soil layers and a negative relationship in deep soil layers. The CO_2 fluxes from CGM and chamber methods had good agreement at multiple time scales, which showed that the CGM method was able to estimate near-surface soil CO_2 fluxes and production. The contrasting patterns between surface and deep layers of soil CO_2 concentration and fluxes suggest the necessity of intensive CO_2 concentration measurements in the surface soil layer for accurate determination of soil-atmosphere CO_2 flux when using the CGM.

Abbreviations: CGM, concentration gradient method.

Soil surface CO_2 emissions are an important element of the terrestrial C cycle. Carbon dioxide concentrations and production in subsurface soil have important impacts on an array of biological processes occurring in a wide range of settings. Soil CO_2 flux with time and depth provides both CO_2 emission estimates from the soil surface and CO_2 production rates with depth in the soil profile.

The concentration gradient method (CGM), based on Fick's law of diffusion, is a technique for estimating the dynamics of CO_2 fluxes and CO_2 production within the soil profile and at the soil surface by determining the concentration gradient and gas diffusivity coefficient (D_s). Alternately, the chamber method directly measures CO_2 flux across the soil surface by measuring the CO_2 concentration change within a closed chamber in a short time. The chamber method cannot provide direct information about production and fluxes with depth. The CGM has disadvantages, with uncertainties for determination of the concentration gradient and D_s (Kusa et al., 2008). However, because the spatial scales of both the CGM and chamber methods are small (within 1 m^2) and both can be used to provide hourly CO_2 fluxes, the CGM, combined with the reference chamber

Soil Sci. Soc. Am. J. 79:1073–1083
doi:10.2136/sssaj2015.02.0079
Received 24 Feb. 2015.
Accepted 4 May 2015.
*Corresponding author (jlheitman@ncsu.edu).

method for validation, has gained wide application in the estimation of soil CO_2 efflux and production in different soil settings (see the review by Maier and Schack-Kirchner, 2014). Some applications of this approach include agricultural fields (Chen et al., 2005; DeSutter et al., 2008; Pingintha et al., 2010), forests (Davidson and Trumbore, 1995; Tang et al., 2005; Jassal et al., 2005; Pumpanen et al., 2008; Sullivan et al., 2010), grasslands (Tang et al., 2003; Sanderman and Amundson, 2010; Verma and Kelleners, 2012), and laboratory soil columns (Turcu et al., 2005; Fan and Jones, 2014). The CO_2 measurements are typically made at approximately three to five soil depths, with one depth, or at most two, being in the 0- to 10-cm soil layer.

The CO_2 concentration profiles and CO_2 flux measurements in the surface soil layer are complex. The interplay of biological, physical, and chemical processes varies considerably in both space and time. Soil temperature and water content are the two main biophysical factors controlling CO_2 production, both of which are highly dynamic in the shallow layer. Carbon dioxide concentration profiling in the near-surface layer is characterized by low concentrations and high transport (diffusion) rates compared with deeper soil layers. It has been reported that the diurnal patterns of CO_2 concentration are out of phase with the soil temperature in surface soil layers (Tang et al., 2003; Pingintha et al., 2010). An opposite diurnal pattern of CO_2 flux relative to soil temperature between surface and deep soil depths was also observed in bare soil, with the underlying mechanism remaining unclear (Pingintha et al., 2010). These variables impose great challenges in deriving CO_2 concentration profiles and CO_2 fluxes if information is known only for limited depths. DeSutter et al. (2008) used six methods to estimate CO_2 concentration gradients and three models to predict diffusion coefficients and found that with some, CGM CO_2 fluxes were >100 times larger than the CO_2 fluxes measured by an automated chamber on the soil surface. High-resolution, finer scale CO_2 concentration measurements in the surface soil layer could help improve the accuracy and gain insight into CO_2 production and transport in this complex zone.

To accurately measure and better understand near-surface soil CO_2 fluxes and soil CO_2 production rates with time and depth, the CGM was used to estimate soil CO_2 fluxes with time and depth in a bare field. The bare soil, with only heterotrophic respiration, exhibited less complex diurnal patterns of CO_2 concentration and flux. We measured soil CO_2 concentration at 13 depths, from the surface to a depth of 200 mm, with a high resolution of eight depths in the top 50 mm, during a natural wetting and drying period. In situ measurements of soil water content and soil temperature near the CO_2 concentration measurements were also made. In parallel measurements, surface CO_2 efflux was also determined with chamber systems for comparison with the CGM flux. The general objective of this study was to better understand near-surface dynamic CO_2 flux and its mechanisms and to model CO_2 concentration and flux with time and depth using the high-resolution measurements. The specific aims of this study were: (i) to determine bare-soil CO_2 fluxes and production rate with time and depth using the CGM, (ii) to investigate the impacts of temperature and moisture on CO_2 production in each layer, and (iii) to compare surface CO_2 effluxes determined by the CGM with chamber measurements.

METHODS AND INSTRUMENTS

Site Description

The study was performed in a 125- by 125-m bare field located near Ames, IA (41.98° N, 93.68° W) during the summer of 2008. The soil at the site was a Canisteo clay loam (a fine-loamy, mixed, superactive, calcareous, mesic Typic Endoaquoll). Soil bulk densities were 1.20 and 1.32 Mg m^{-3} in the surface soil layer (0–60 mm) and 60- to 120-mm soil layers, respectively. The soil consisted of 44, 30, and 26% sand, silt, and clay, respectively, and the topography was relatively flat (slope <2%). Before this study the field was tilled, and during the study it was kept bare by spraying herbicides to control plant growth.

Gradient Method for Determining Carbon Dioxide Fluxes

Thirteen solid-state sensors (GMT 222 and GMT 221, Vaisala) with three measurement ranges (GMT 221, 0–1%; GMT 221, 0–3%; GMT 222, 0–10%) were used to measure the CO_2 concentration from the soil surface to the 200-mm depth. The sensors assess the CO_2 concentration by detecting the attenuation of single-beam dual-wavelength infrared light across a certain distance. Probes with a range of 0 to 1% were buried at depths of 0 and 3 mm, probes with a range of 0 to 3% were buried at depths of 9, 15, 21, 27, 33, 45, 57, and 75 mm, and probes with a range of 0 to 10% were buried at depths of 100, 150, and 200 mm (Fig. 1d). For probe installation, a narrow trench was dug, a probe was placed horizontally at a selected depth and the probe was covered with soil. A CO_2 analyzer (SBA-4, PP Systems) was used as a standard to calibrate all of the solid-state sensors before installation. Each sensor was calibrated at five CO_2 concentrations in a laboratory chamber.

The solid-state CO_2 sensors consisted of three parts: a remote probe, a transmitter body, and a cable connecting the probe to the transmitter (Fig. 1a). The probes are cylindrical with a length of 15.5 cm and a diameter of 1.85 cm. There are six narrow slits around the probe to allow CO_2 to diffuse into the sensor. To gain more precise measurement in the soil, we covered four of the six slits with 3M 5413 polyimide film tape (Fig. 1b) (one slit at the bottom view and three slits at the top view of the probe were covered). By keeping only two probe slits open, the vertical sampling thickness for each probe was limited to 5 mm. Each probe was covered with a porous Teflon cap that allowed CO_2 gas to move freely into the uncovered probe slits but prevented water from entering the probe. Probes were connected to a 24-V direct current (DC) power source (two rechargeable batteries connected in series, and each battery recharged by one 12-V solar panel) and a datalogger that recorded the CO_2 concentrations by measuring the voltage signal of the probes. Two 21X dataloggers (Campbell Scientific) were used to control and monitor the 13

buried sensors in this study. To conserve power and avoid heating of the surrounding soil, a relay was used to regulate the 24-V DC power source with 10 min on (including ab 8-min warm-up time and 2-min measurement time) and 50 min off each hour. The average CO_2 concentration during the 2-min measurement period for each probe was recorded. The transmitter bodies and dataloggers were protected from environmental conditions by keeping them in a plastic box in the field.

Using measured CO_2 concentrations, CO_2 fluxes (F_{CO2}) at various soil depths were calculated using Fick's law of diffusion:

$$F_{CO_2} = -D_s \frac{dC}{dz} \quad [1]$$

where D_s and dC/dz represent the soil gas diffusion coefficient and CO_2 concentration gradient, respectively. To improve the accuracy of the concentration gradient, CO_2 concentrations across all depths were fitted with a quadratic model. The quadratic model of CO_2 concentration with depth is

$$C(z) = az^2 + bz + c \quad [2]$$

where C denotes concentration, z the depth, and a, b, and c are fitted parameters. The concentration gradient was accordingly determined hourly with the following quadratic model:

$$\frac{dC}{dz} = 2az + b \quad [3]$$

We obtained D_s with the Millington and Quirk (1961) model (referred to here as the MQ1961 model) and five other empirical models (Penman, 1940; Marshall, 1959; Moldrup et al., 1997, 1999, 2000) and evaluated all the models according to the goodness-of-fit between gradient-based soil-atmosphere CO_2 flux and the chamber-based reference method. The results indicated that the MQ1961 model in combination with the above quadratic model for concentration gradient gave the best CO_2 flux when compared with the reference chamber measurements. Thus, D_s was estimated with the MQ1961 model, including a temperature (T, °C) effect:

$$D_s = (D_a)\frac{\varepsilon^{10/3}}{\Phi^2}\left(\frac{273.15+T}{295.15}\right)^{1.75} \quad [4]$$

$$\Phi = 1 - \frac{\rho_b}{\rho_s} \quad [5]$$

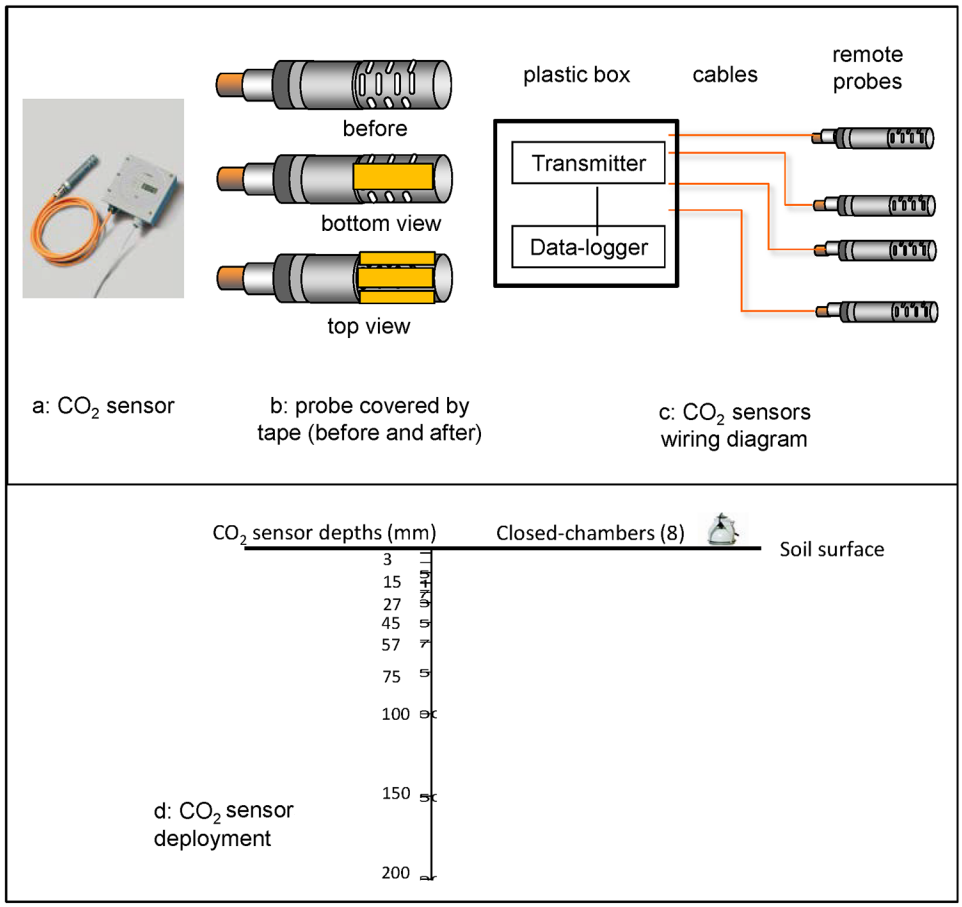

Fig. 1. Configuration of CO_2 solid sensors and installations in the ground.

$$\varepsilon = \Phi - \theta \quad [6]$$

where D_a is the CO_2 diffusion coefficient in free air (16×10^{-6} m^2 s^{-1}). Total porosity Φ was calculated from the measured soil bulk density (ρ_b, Mg m^{-3}) and assumed particle density (ρ_s = 2.65 Mg m^{-3}) (Eq. [5]), and air-filled porosity ε was calculated from the volumetric water content (θ) and Φ (Eq. [6]).

Heat-pulse sensors (Xiao et al., 2014) were installed in the soil 1 m from the buried CO_2 sensors, to determine θ (Fig. 2). Volumetric water content θ was derived from the volumetric heat capacity of the soil (C_v, J m^{-3} K^{-1}), which was measured by the heat-pulse method (Knight and Kluitenberg, 2004), specific heat capacity of solids (C_s = 0.85 J g^{-1} K^{-1}), soil bulk density ρ_b, water density (ρ_w = 1 Mg m^{-3}), and the volumetric heat capacity of water (C_s = 4.17 MJ m^{-3} K^{-1}):

$$C_v = C_s\rho_b + \rho_w C_w\theta \quad [7]$$

where soil temperatures between the surface and the 48-mm soil depth were measured with chromel-constantan (Type E) thermocouples within the heat-pulse sensors, and T between the 48- and 200-mm soil depths was measured by independent Type E thermocouples buried within the soil, also 1 m from the CO_2 sensors.

Carbon dioxide produced within a soil layer (P_{CO2}) can be estimated from the net soil layer CO_2 flux [the difference of F_{CO2} at upper and lower boundaries of a soil layer, $(F_{CO2})_1$ –

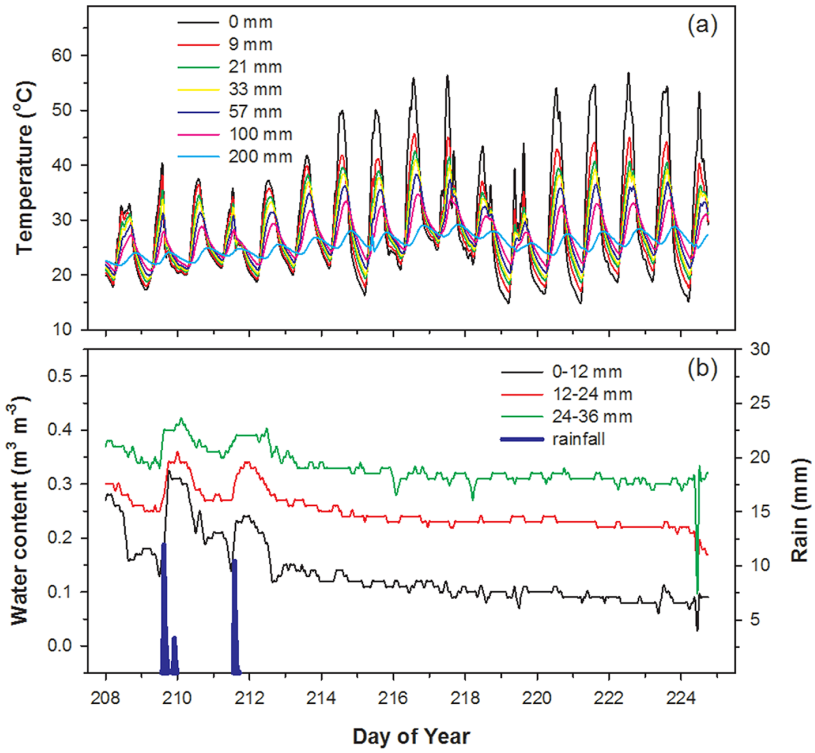

Fig. 2. Soil (a) temperature and (b) water content at various depths.

$(F_{CO2})_2$] and the change in the storage of CO_2 (ΔS_{CO2}) in the soil layer:

$$P_{CO_2}=\left[\left(F_{CO_2}\right)_1-\left(F_{CO_2}\right)_2\right]+\Delta S_{CO_2} \quad [8]$$

The amount of CO_2 stored in a soil layer is relatively small compared with F_{CO2}, so the P_{CO2} in a soil layer was estimated from the difference in cumulative CO_2 emitted at the soil layer boundaries (Risk et al., 2002).

Temperature and Water Content Sensitivity of Soil Carbon Dioxide Production

The effect of soil temperature on soil CO_2 production was evaluated by the following commonly used empirical model (e.g., Davidson et al., 1998; Pingintha et al., 2010; Verma and Kelleners, 2012):

$$F(T)=S_0\exp(\beta T) \quad [9]$$

where $F(T)$ denotes soil CO_2 efflux as a function of T, S_0 is the reference soil CO_2 flux at 0°C, and β, a parameter related to the Q_{10} coefficient, is determined by fitting Eq. [9] to data. The Q_{10} coefficient is determined as

$$Q_{10}=\exp(10\beta) \quad [10]$$

To better assess the effect of soil water content on soil CO_2 flux at a given depth, soil CO_2 flux is normalized by temperature first and then used to fit a linear or quadratic function. The normalization is achieved by dividing the measured CO_2 flux by the best-fit values from Eq. [9]. The linear model we used is (Pingintha et al., 2010)

$$\frac{F_{s,e}}{F(T)}=m\theta+n \quad [11]$$

In light of previous studies, θ could have two opposite effects on soil respiration (Tang et al., 2005; Verma and Kelleners, 2012) in that soil that is too dry or too wet can reduce soil CO_2 production. Hence, a quadratic model was also used for parameter fitting:

$$\frac{F_{s,e}}{F(T)}=f\theta^2+g\theta+h \quad [12]$$

where $F_{s,e}$ is the measured CO_2 efflux at each layer. Parameters m and n in Eq. [11] and f, g, and h in Eq. [12] require fitting.

Chamber Measurements for Carbon Dioxide Flux

Eight long-term chambers (LI-8100–104, LI-COR) were installed in a linear transect 3.5 m apart to automatically measure bare-soil surface CO_2 efflux. The soil CO_2 sensors were installed at a distance of about 1 m from the midpoint of the linear transect of the eight chambers. The eight chambers were connected to an infrared gas analyzer (LI-8100) system and a multiplexer (LI-8150), which were both powered by a power supply (LI-8150-770) connected to 110 alternating current (AC) power in the field. The polyvinyl chloride collars (with a height of 11.4 cm and a diameter of 20.3 cm) were inserted in the soil with a 2- to 4-cm height of each collar above the soil surface. The combined LI-8100 and LI-8150 multiplexer system controlled the CO_2 flux measurements. The analyzer measured CO_2 concentrations when the chambers were closed, and the concentration change with time was then used to calculate the CO_2 flux. Measurements on the eight chambers were performed sequentially for 16 min every hour, with 2 min for each chamber (including 25-s deadband time and 45-s purge time).

RESULTS AND DISCUSSION

Carbon Dioxide Concentration Measurements in the Soil Profile

Soil CO_2 concentrations at various depths in the 0- to 200-mm soil layer were measured from 28 July (DOY 209) to 8 August (DOY 223) in the summer of 2008. There were two rainfall events during the measurement period (DOY 209, 23 mm, and DOY 211, 14 mm). Figure 3 shows the measured hourly CO_2 concentrations at various soil depths: the surface to 9-mm soil depth concentrations are in Fig. 3a, the 15- to 45-mm soil depth concentrations are in Fig. 3b, and the concentrations below 45 mm are in Fig. 3c. Carbon dioxide concentrations increased with soil depth. The CO_2 concentration values were <0.12% at the 0- and 3-mm soil depths, ranged from 0.02 to 0.2% at the 9-mm soil depth, from 0.1 to 2.1% at soil depths between 15

and 45 mm, from 0.2 to 2.2% at soil depths between 57 and 100 mm, and from 0.8 to 2.4% at depths of 150 and 200 mm. Soil CO_2 concentrations exhibited diurnal changes at all soil depths, with a larger amplitude in deeper soil layers. Because there were very few living roots in the bare field, soil microbial respiration was the main source of CO_2.

Figure 4 shows the daily mean values of CO_2 concentrations as the soil dried from DOY 213 to 223. Mean concentration values increase slowly with depth in the 0- to 33-mm soil layer and then increase relatively quickly with depth in the 45- to 200-mm layer. Carbon dioxide concentrations were not statistically different from 21 to 27 mm, and there was a slight decline from 27 to 33 mm. A possible reason for similar concentrations in the 0- to 30-mm layer of soil is that rapid gas transport in this zone prevents CO_2 accumulation. The concentration gradient for the whole layer has a concave shape, with a slope less than that for a linear function (Fig. 4). Concentration gradient values for deeper soils have been reported previously in different soil ecosystems and modeled with power, quadratic, exponential, and sigmoid functions. The CO_2 concentration profiles with depth in previous studies were depicted as convex shapes, with slopes greater than for a linear function (see the review by Maier and Schack-Kirchner, 2014). The relatively slow increases in surface soil layers in the current work may be site specific to the bare-soil study site under drying conditions. It may also reflect the real CO_2 concentration profile in the surface soil layer, undetected due to the absence of CO_2 sensor installation at such shallow depths in earlier studies.

Soil Carbon Dioxide Fluxes and Production with Time and Depth

There were no obvious soil CO_2 concentration increases observed in the 0- to 3-mm soil layer, but large CO_2 concentration increases were observed at 9 mm and below during the rainfall events and 1 d after. This indicates that surface sealing may prevent CO_2 escaping from the soil and increase subsurface CO_2 concentrations (Chen et al., 2005; Jassal et al., 2005; DeSutter et al., 2008). Fick's law is not able to accurately describe the CO_2 movement in the soil during these rainy days because the surface soil was sealed with water and the air porosity varied significantly with depth in the soil profile.

Soil CO_2 concentration distribution was influenced by rainfall. Carbon dioxide concentrations at 9 mm and below increased immediately after each rainfall event, reached maximum values about 1 d after a rainfall event, decreased rapidly 1 d later, and then slowly decreasing as the soil dried. Rain did not

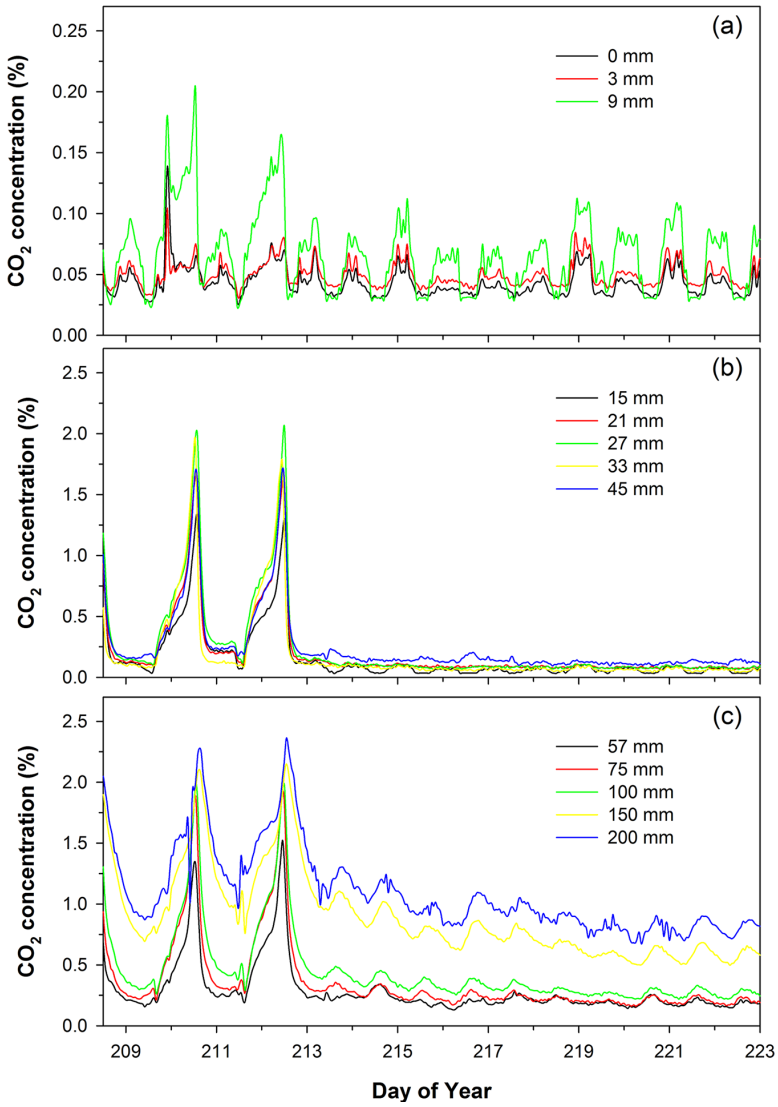

Fig. 3. Carbon dioxide concentrations measured at (a) 0 to 9 mm, (b) 15 to 45 mm, and (c) 57 to 200 mm as measured by CO_2 sensors.

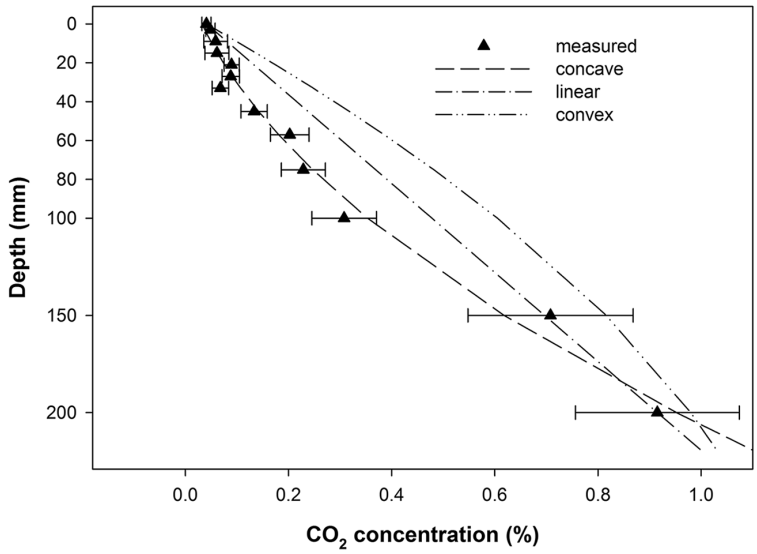

Fig. 4. Carbon dioxide concentrations at various depths (error bars are standard deviations of 11 daily means). An overall concave curvature of CO_2 concentration in this study is different from the convex curvatures in previous studies.

cause CO_2 concentrations to increase at the 0- and 3-mm soil depths due to the proximity of the soil–atmosphere interface and because most of the pores were occupied by water from rainfall. The large increase in soil CO_2 concentration at 9 mm soon after the rainfall events may be caused by surface sealing, by the wet soil surface layer decreasing gas diffusion between the soil and atmosphere, and/or by increased CO_2 production due to enhanced microbial activity in the wetted soil (Chen et al., 2005; Jassal et al., 2005; DeSutter et al., 2008). Following the rainfall, CO_2 concentrations at the 9-mm depth and below began to decrease because the soil was drying, which increased the air-filled pore space, enabling CO_2 gas diffusion from the deep soil to the surface.

Soil CO_2 fluxes during the soil drying period (DOY 213–223) were estimated from the fitted CO_2 concentrations and estimated gas diffusion coefficients at different soil depths with the CGM. Different CO_2 diffusivity models were tested, and the goodness-of-fit models were chosen from each layer. The MQ1961 model gave the best results and is thus the only model included here. Carbon dioxide fluxes with time and depth are shown in Fig. 5. Carbon dioxide fluxes at the top depths (1.5-, 6-, 9-, 12-, 18-, 24-, and 30-mm soil depths) are shown in Fig. 5a. Fluxes at the 51-, 66-, 87.5-, 125-, and 175-mm soil depths are shown in Fig. 5b. The CO_2 fluxes showed diurnal variations in the 0- to 66-mm soil layer, and the diurnal variations diminished with soil depth. At the 1.5-mm soil depth, large variation in the CO_2 fluxes was observed, with values ranging from 1 to 8 μmol m^{-2} s^{-1}. The variation was relatively stable during the measurement period. At soil depths from 1.5 to 66 mm, significant diurnal variations were also observed (Fig. 5). The values of CO_2 flux ranged from 1 to 8, 0 to 5, and 0 to 0.4 μmol m^{-2} s^{-1} at soil depths of 12 mm and above, 18 to 30 mm, and 51 mm and below, respectively. At soil depths from 1.5 to 40 mm, the diurnal fluctuation of CO_2 fluxes decreased from a peak value of 7 to 0.5 μmol m^{-2} s^{-1}. At a soil depth of 50 mm and below, CO_2 fluxes were stable at approximately 0.4 μmol m^{-2} s^{-1}. The CO_2 flux distributions indicated that CO_2 diffused from the soil to the atmosphere and the CO_2 production rates varied with soil depth.

Carbon Dioxide Production with Time and Depth and Its Correlation with Temperature and Water Content

Figure 5c shows the cumulative CO_2 fluxes emitted at various soil depths during the soil drying period from DOY 213 to 223. During the 11-d soil drying period, the average cumulative emitted CO_2 was 3.8 mol m^{-2} at the soil surface from the chamber measurements, and the cumulative emitted CO_2 was 3.8, 3.3, 3.0, 2.2, 0.6, 0.2, 0.1 mol m^{-2} at soil depths of 0 (linear extrapolation), 1.5, 6, 12, 24, 51, and 175 mm, respectively, from the CGM. The CO_2 flux at the soil surface modeled from linear extrapolation agreed very well with the chamber-measured CO_2 flux at the soil surface. The cumulative CGM CO_2 emitted at the 1.5-mm soil depth underestimated the chamber surface CO_2 flux by 13%.

Carbon dioxide fluxes varied with depth because CO_2 production rates varied with depth. Most of the CO_2 was produced in shallow soil depths in this bare field. A small portion (2%) of the CO_2 was produced below a depth of 175 mm, 8% was produced in the 50- to 175-mm soil layer, and 90% was produced in the 0- to 50-mm soil layer. Nakadai et al. (2002) reported that 70% of CO_2 was produced in the 0- to 100-mm soil layer in a bare field in Japan. The reason that Nakadai et al. (2002) had lower CO_2 production in the 0- to 100-mm soil layer might be

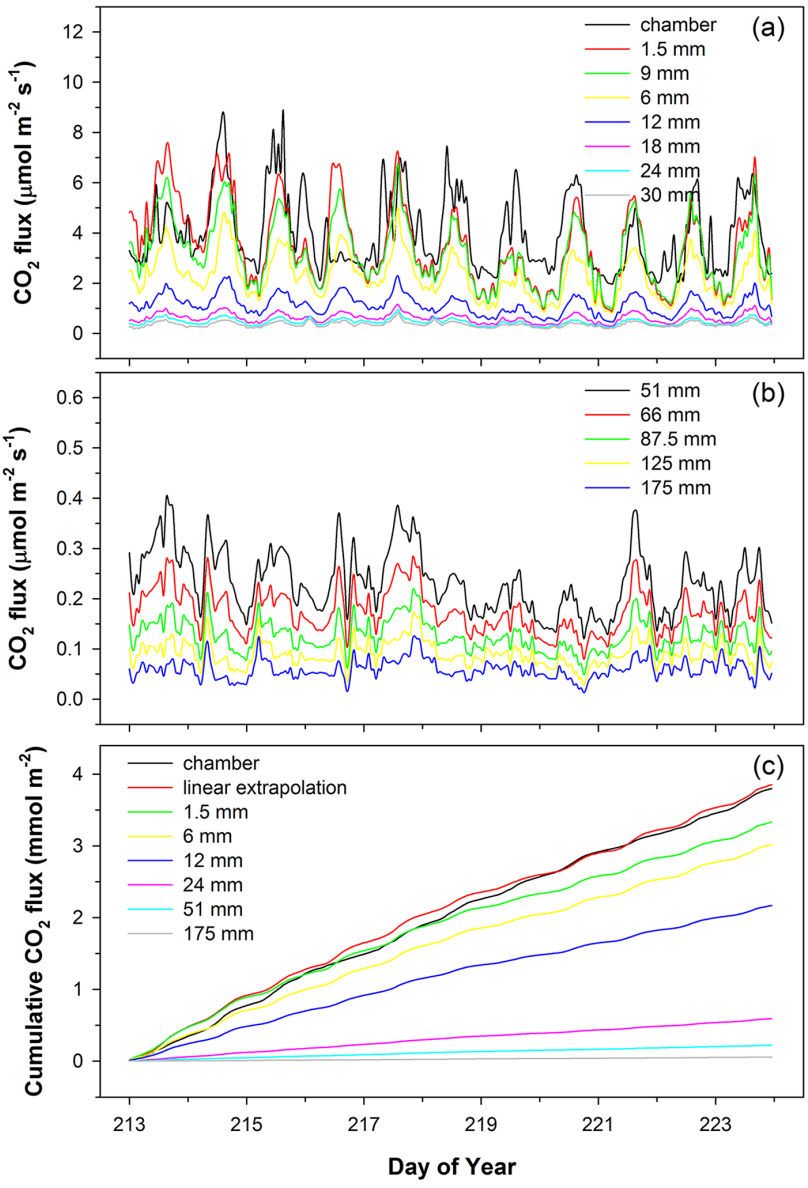

Fig. 5. Soil CO_2 fluxes for (a) chamber measurements and 1.5- to 30-mm depths with the concentration gradient method (CGM) and (b) 51- to 175-mm depths with CGM and (c) cumulative soil CO_2. Linear extrapolation was based on depths of 6 and 12 mm.

that their field was maintained bare for a longer time (>20 yr) than this bare field (2 yr), and another potential reason might be the difference in the soil texture at the two locations. The low percentage of production in deep layers in this work may be attributed to the unfavorable wet conditions and lower temperature in deeper soil layers.

Soil CO_2 production can be interpreted by correlation with environmental factors including soil temperature, water content, and precipitation. The soil temperature sensitivity can be expressed by fitting parameters to an exponential function. The coefficients that represent temperature sensitivity at each depth are given in Table 1. Soil CO_2 effluxes from most of the soil layers can be well described by an exponential function of soil temperature, with temperature sensitivity (Q_{10}) ranging from 1.40 to 2.00 (1.62 ± 0.17). The correlation coefficients range from 0.29 to 0.84. The 6- to 12- and 39- to 51-mm layers are shown as examples in Fig. 6. A range of Q_{10} values of 1.24, 1.81, to 2.23 in the top 20, 50, and 120 mm was reported in a peanut (*Arachis hypogaea* L.) field (Pingintha et al., 2010).

Tables 2 and 3 summarize the sensitivity of soil CO_2 production to water content, normalized by soil temperature. Overall, a quadratic relationship of temperature-normalized CO_2 flux responding to soil water content has a comparable or slightly better fit than a linear relationship. In some layers, acceptable correlation coefficients (R^2 > 0.40) suggest that temperature-normalized soil CO_2 effluxes can be partly explained by soil water content. The soil was relatively wet due to the two major rainfall events (DOY 209 and 211), with water content >0.1 m^{-3} m^{-3}at the soil surface and increasing with depth. There exists a positive linear relationship between temperature-normalized CO_2 flux and water content in surface, dry soil layers and a negative linear relationship in the deep, wet soil layers. Figure 6 gives two representative layers to illustrate this opposing effect of soil water content. By depthwise comparison and visual identification, the optimal water content for CO_2 production in our work can be roughly identified as 0.30, close to field capacity for this bare field. Luo and Zhou (2006) indicated that the optimal water content for microbial activity usually occurs near field capacity.

Table 1. Parameter fitting of soil temperature to CO_2 efflux in soil layers using Eq. [9].

Depth	11-d cumulative production	Parameter estimation			Evaluation measures		
		S_0	β	Q_{10}	R^2	NSE†	RMSE
mm	mmol m^{-2}						
0 (1.5)–6	86.58	0.11	0.03	1.40	0.29	0.08	0.47
6–12	236.13	0.21	0.05	1.60	0.79	0.62	0.30
12–18	302.75	0.29	0.05	1.59	0.84	0.70	0.27
18–24	135.00	0.11	0.05	1.65	0.79	0.62	0.14
24–30	43.49	0.03	0.06	1.75	0.82	0.68	0.04
30–39	25.69	0.03	0.04	1.44	0.54	0.29	0.03
39–51	33.65	0.02	0.07	1.99	0.58	0.34	0.07
51–66	15.71	0.01	0.05	1.69	0.73	0.53	0.02
66–88	12.61	0.01	0.05	1.64	0.67	0.45	0.01
88–125	9. 31	0.01	0.05	1.66	0.61	0.38	0.01
125–175	8.19	0.01	0.04	1.43	0.42	0.18	0.01
>175	15.75						

† Nash–Sutcliffe efficiency coefficient.

Diurnal Variations of Soil Temperature and Carbon Dioxide Concentration and Flux

Soil temperature and CO_2 concentration and flux during the 11 drying days in the study period were averaged to a 24-h daily diurnal pattern. All of the diurnal patterns are plotted by depth in Fig. 7.

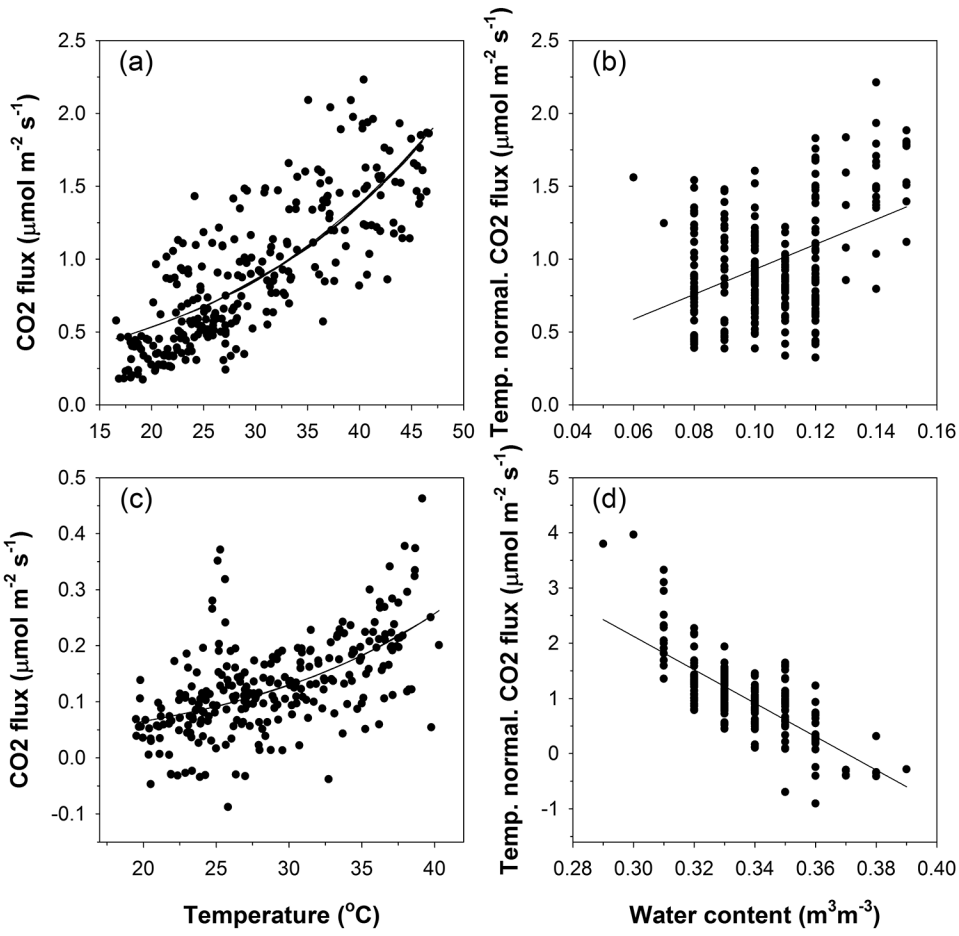

Fig. 6. (a,c) Soil temperature effects on soil efflux and (b,d) water content effects on temperature-normalized soil efflux in the (a,b) 6- to 12-mm layer where soil is relatively dry and (c,d) 39- to 51-mm layer where the soil is wet.

Table 2. Parameter fitting of soil water content to temperature-normalized CO_2 flux using a linear model to fit $F_{s,e}/F(T) = m\theta + n$, where $F_{s,e}$ is the measured CO_2 efflux at each layer, $F(T)$ is the soil CO_2 efflux as a function of temperature T, and θ is the volumetric water content.

	Parameter estimates		Evaluation measurements		
Depth	*m*	*n*	R^2	NSE†	RMSE
mm					
0 (1.5)–6	11.60	−0.05	0.13	0.02	1.40
6–12	8.57	0.07	0.41	0.17	0.33
12–18	3.62	0.42	0.25	0.06	0.23
18–24	10.28	−1.42	0.45	0.20	0.25
24–30	4.31	−0.26	0.21	0.04	0.27
30–39	14.48	−3.58	0.52	0.27	0.31
39–51	−30.29	11.21	0.73	0.53	0.43
51–66	−1.76	1.65	0.07	0.00	0.26
66–88	−3.77	2.46	0.15	0.02	0.24
88–125	−4.87	2.99	0.20	0.04	0.24
125–175	−9.37	5.01	0.45	0.20	0.18
>175					

† Nash–Sutcliffe efficiency coefficient.

Table 3. Parameter fitting of soil water content to temperature-normalized CO_2 flux using the equation $F_{s,e}/F(T) = f\theta^2 + g\theta + h$, where $F_{s,e}$ is the measured CO_2 efflux at each layer and $F(T)$ is the soil CO_2 efflux as a function of temperature T.

	Parameter estimates			Evaluation measurements		
Depth	*f*	*g*	*h*	R^2	NSE†	RMSE
mm						
0 (1.5)–6	220.4	−25.5	1.5	0.15	0.02	1.40
6–12	369.7	−72.5	4.4	0.56	0.32	0.30
12–18	−22.4	11.1	−0.2	0.26	0.07	0.23
18–24	114.0	−44.6	5.2	0.46	0.21	0.25
24–30	113.5	−62.5	9.5	0.23	0.05	0.27
30–39	276.2	−160.9	24.2	0.57	0.32	0.30
39–51	286.8	−225.4	44.3	0.75	0.56	0.41
51–66	−80.5	57.9	−9.4	0.08	0.01	0.26
66–88	−76.4	55.9	−9.2	0.16	0.03	0.24
88–125	−89.4	68.5	−12.1	0.20	0.04	0.24
125–175	−15.6	4.0	2.1	0.45	0.20	0.18
>175						

† Nash–Sutcliffe efficiency coefficient.

Depthwise comparison of the diurnal patterns of soil CO_2 concentration relative to soil temperature showed that CO_2 concentrations in surface soil layers exhibited a diurnal trend that was out of phase relative to soil temperature, whereas the diurnal trends of temperature and CO_2 production were in phase in the deeper soil (Fig. 3). Carbon dioxide concentrations showed clear diurnal variation, with a contrasting phase to soil temperature in the surface soil depths (0, 3, 9, and 15 mm), and followed the same diurnal trend as temperature in relatively deep soil depths (57, 75, 100, 150, and 200 mm). In soil depths in between (21, 27, 33, and 45 mm), the concentration showed a moderate diurnal trend, and a shift can be observed in this transitional zone. The patterns of the CO_2 concentrations below the 33-mm soil depth (Fig. 7, 3b, and 3c) were similar to the surface soil temperature (Fig. 2a), with the values increasing in the early morning, reaching a maximum value in the early afternoon, and decreasing to a minimum value near midnight. However, the pattern of the CO_2 concentrations between 0 and 33 mm (Fig. 3a) was out of phase with the surface soil temperature, with peak values occurring in the night and low values occurring in the daytime. Relatively large CO_2 concentrations observed in the daytime below the 33-mm depth were due to enhanced soil microbial activity with high temperatures. Possible reasons for the low CO_2 concentrations in the daytime and large nighttime CO_2 concentrations in the shallow soil may be due to greater diffusivity (i.e., a larger CO_2 diffusion coefficient) in the 0- to 33-mm soil layer preventing CO_2 buildup in the early afternoon. In the early afternoon, the atmospheric CO_2 concentrations above the surrounding cropped fields were relatively low due to photosynthesis. Flux tower measurements indicated that the CO_2 concentrations at night were sometimes two times larger than the CO_2 concentration in the afternoon (data not shown). The atmospheric CO_2 concentration above the bare field might be underestimated because the atmosphere above the bare field was well mixed with the surrounding corn (*Zea mays* L.) field atmosphere, resulting in a large concentration gradient from soil to atmosphere early in the afternoon. Carbon dioxide production rates may also decrease as the soil temperature exceeds a certain temperature. Carbon dioxide production rates are sensitive to high soil temperature. The soil surface temperature exceeded 50°C in the early afternoon, a temperature that may inhibit the growth of bacteria, and decreased CO_2 production rates. Tang et al. (2003) and Pingintha et al. (2010) observed a similar soil CO_2 concentration distribution pattern. Both groups found that the CO_2 concentration at 20 mm had a diurnal trend opposite to that of the surface soil temperature, while the CO_2 concentration at the 80- and 160-mm (Tang et al., 2003) and 120-mm (Pingintha et al., 2010) soil depths had the same diurnal trends as the surface soil temperature.

Several possibilities exist to account for the out-of-phase diurnal trend between CO_2 flux and CO_2 concentration in the top layer. The above-mentioned exaggerated gradient-driven CO_2 transport from near surface to atmosphere may be one of the reasons. The top 33-mm zone marks a high CO_2 production yet low concentration and low concentration gradient zone, suggesting high CO_2 transport in this zone.

Carbon dioxide fluxes in topsoil layers reached the peaks of diurnal curves later than soil temperature but earlier than the soil temperature in deeper soil layers. Pingintha et al. (2010) also reported contrasting CO_2 flux shifts in response to temperature between shallow and deep soil layers in a bare-soil ecosystem. These findings suggest a more complex process of CO_2 flux in near-surface soils and that further study is needed.

Comparing Gradient Method Derived Soil Carbon Dioxide Effluxes with Chamber Carbon Dioxide Surface Effluxes

As soil CO_2 concentrations were being measured, CO_2 effluxes were measured automatically with eight chambers in

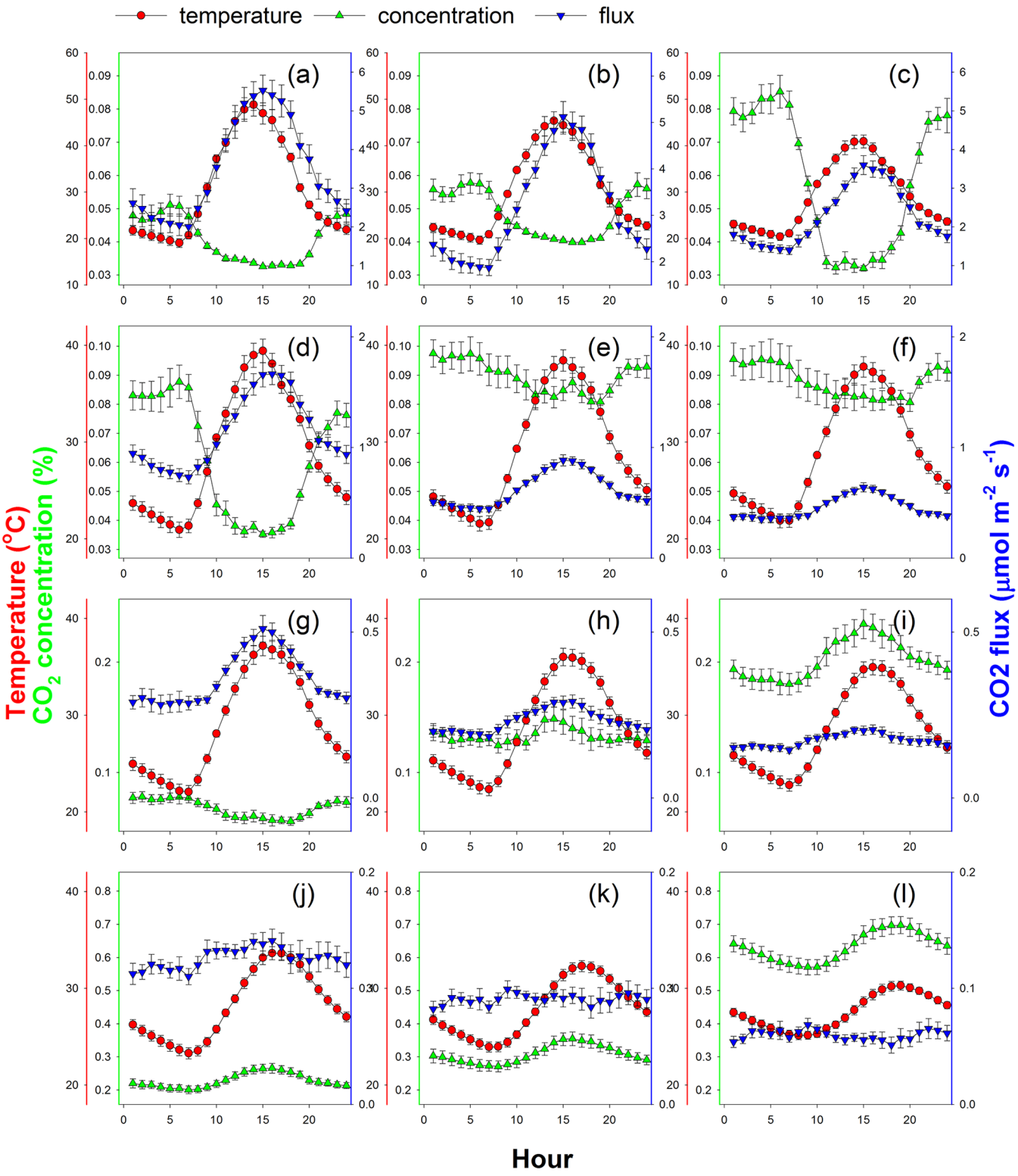

Fig. 7. Diurnal variations of soil temperature and CO_2 concentration and efflux in the different soil layers (from shallow depth to deep) at depths of (a) 0, (b) 3, (c) 9, (d) 15, (e) 21, (f) 27, (g) 33, (h) 45, (i) 57, (j) 75, (k) 100, and (l) 150 mm.

the bare field from DOY 213 to 223. The CGM CO_2 flux at the shallowest depth of 1.5 mm was compared with the CO_2 effluxes measured by the surface chambers. In addition, surface CO_2 efflux was also derived from linear extrapolation of two near-surface depths, 6 and 12 mm, and compared with the chamber measurements.

The CGM and chamber (average CO_2 effluxes of the eight chambers) hourly CO_2 fluxes are shown in Fig. 8a. The diurnal fluctuations derived from the fitted CGM (dC/dz) of CO_2 flux tracked very well with the chamber diurnal fluctuations, with large peaks occurring early in the afternoon and low peaks occurring during midnight of each day. Using fitted concentration

gradients eliminated the out-of-phase issue at the surface soil layer caused by approximating the concentration gradient as the difference of CO_2 concentrations divided by the depth difference. We also compared daily average values of CO_2 fluxes calculated from the CGM with the mean and standard deviation values of the daily average CO_2 flux from the eight chambers (Fig. 8b). We observed some variation in the eight chambers, with the standard deviation ranging from 0.61 to 2.52 μmol m^{-2} s^{-1} and the CV ranging from 28 to 52% during the measurement period (Table 4). The values of daily CO_2 flux from the CGM were all within the range of one standard deviation of the average of the eight chambers. The cumulative CO_2 flux during the study period also showed good agreement, with the linear extrapolated surface fluxes better matching the chamber surface fluxes than the 1.5-mm flux (Fig. 5c).

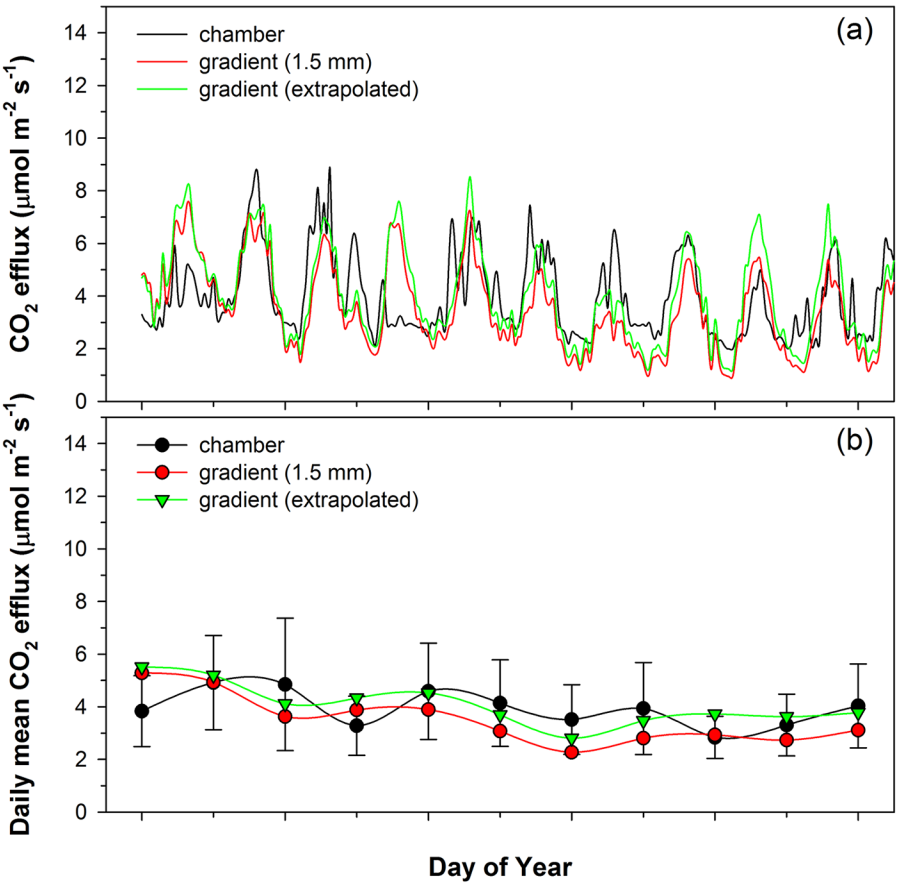

Fig. 8. (a) Diurnal CO_2 fluxes from the chamber method (average of eight chambers), the modeled gradient method at 1.5 mm and linear extrapolation, and the measured gradient method at 1.5 mm; and (b) daily mean CO_2 fluxes from eight chambers (error bars are stand deviations), the gradient method at 1.5 mm, and linear extrapolation. Linear extrapolation was based on measurements at 6 and 12 mm.

CONCLUSIONS

Soil CO_2 concentrations, fluxes, and production rates in the near-surface soil layers were determined with the CGM method at high resolution and validated by surface chamber measurements. Soil CO_2 concentrations increased and fluxes decreased with soil depth. Carbon dioxide concentrations in the shallow soil layers (within 33 mm) show a concave curvature, which has not been reported in the literature. Only 2% of the cumulative soil CO_2 was produced below a depth of 175 mm, 8% was produced in the 50- to 175-mm soil layer, and 90% was produced in the 0- to 50-mm soil layer.

Soil CO_2 effluxes from most soil layers can be well described by an exponential function of soil temperature, with temperature sensitivity (Q_{10}) ranging from 1.40 to 2.00 (1.62 ± 0.17). Temperature-normalized soil CO_2 effluxes can further be partly explained as a function of soil water content, with a positive linear relationship in surface, dry soil layers and a negative linear relationship in deep, wet soil layers.

Depthwise comparison of the diurnal patterns of soil CO_2 concentration relative to soil temperature showed that CO_2 concentrations in surface soil layers exhibited a diurnal trend opposite to soil temperature, whereas CO_2 concentrations and soil temperature diurnal trends were more in phase in deeper soil layers. The high-resolution CO_2 concentration measurements enabled a determination of the dynamic shift of such diurnal trends. Carbon dioxide fluxes in surface soil layers reached their peaks late relative to soil temperature, whereas they remained relatively constant in deeper soil layers. The contrasting patterns of CO_2 concentration and CO_2 fluxes between surface and deep layers observed in this study suggest the complexity of soil CO_2 production and transport in the surface soil layer. It also implies the necessity for intensive CO_2 concentration measurements in surface soil layers for accurate inference of soil-atmosphere CO_2 flux. Such contrasting patterns need further tests in other soil ecosystems.

Table 4. Descriptive statistics of CO_2 flux from eight chambers for days of the year (DOY) 213 to 224.

DOY	Mean	Min.	Max.	SD	CV
	μmol m^{-2} s^{-1}				%
213	3.83	2.00	6.52	1.35	35
214	4.92	2.09	6.75	1.79	36
215	4.85	2.11	9.77	2.52	52
216	3.28	1.91	4.88	1.12	34
217	4.59	2.07	6.86	1.83	40
218	4.10	1.55	6.37	1.70	41
219	3.52	1.60	5.41	1.32	38
220	3.92	1.46	6.46	1.76	45
221	2.84	1.60	4.06	0.80	28
222	3.30	1.44	4.95	1.19	36
223	4.01	1.37	6.14	1.64	41
224	2.05	0.96	2.77	0.61	30

The diurnal fluctuations and daily mean and cumulative values of the gradient CO_2 fluxes were similar to the diurnal fluctuations of the chamber fluxes. Thus, the CGM was able to accurately measure bare-field soil CO_2 fluxes and soil CO_2 production with time and depth with the accurate estimation of D_s. Further studies under a range of field moisture and management conditions and long-term measurements are needed to evaluate and improve the determination of vertical CO_2 concentration gradients and in situ CO_2 diffusion coefficients at the soil surface.

ACKNOWLEDGMENTS

This work was supported by the National Science Foundation (Grants no. 0809656 and 1215864) and by the Hatch Act, State of Iowa, and State of North Carolina funds.

REFERENCES

Chen, D., J.A.E. Molina, C.E. Clapp, R.T. Venterea, and A.J. Palazzo. 2005. Corn root influence on automated measurement of soil carbon dioxide concentrations. Soil Sci. 170:779–787. doi:10.1097/01.ss.0000190512.41298.fc

Davidson, E.A., E. Belk, and R.D. Boone. 1998. Soil water content and temperature as independent or confounded factors controlling soil respiration in a temperate mixed hardwood forest. Global Change Biol. 4:217–227. doi:10.1046/j.1365-2486.1998.00128.x

Davidson, E.A., and S.E. Trumbore. 1995. Gas diffusivity and production of CO_2 in deep soils of the eastern Amazon. Tellus B 47:550–565. doi:10.1034/j.1600-0889.47.issue5.3.x

DeSutter, T.M., T.J. Sauer, T.B. Parkin, and J.L. Heitman. 2008. A subsurface, closed-loop system for soil carbon dioxide and its application to the gradient efflux approach. Soil Sci. Soc. Am. J. 72:126–134. doi:10.2136/sssaj2006.0101

Fan, J., and S.B. Jones. 2014. Soil surface wetting effects on gradient-based estimates of soil carbon dioxide efflux. Vadose Zone J. 13(2). doi:10.2136/vzj2013.07.0124

Jassal, R., A. Black, M. Novak, K. Morgenstern, Z. Nesic, and D. Gaumont-Guay. 2005. Relationship between soil CO_2 concentrations and forest-floor CO_2 effluxes. Agric. For. Meteorol. 130:176–192. doi:10.1016/j.agrformet.2005.03.005

Knight, J.H., and G.J. Kluitenberg. 2004. Simplified computational approach for the dual-probe heat-pulse method. Soil Sci. Soc. Am. J. 68:447–449. doi:10.2136/sssaj2004.4470

Kusa, K., T. Sawamoto, R. Hu, and R. Hatano. 2008. Comparison of the closed-chamber and gas concentration gradient method for measurement of CO_2 and N_2O fluxes in two upland field soils. Soil Sci. Plant Nutr. 54:777–785. doi:10.1111/j.1747-0765.2008.00292.x

Luo, Y., and X. Zhou. 2006. Soil respiration and the environment. Academic Press, San Diego.

Maier, M., and H. Schack-Kirchner. 2014. Using the gradient method to determine soil gas flux: A review. Agric. For. Meteorol. 192–193:78–95. doi:10.1016/j.agrformet.2014.03.006

Marshall, T.J. 1959. Gas diffusion in porous media. Science 130:100–102.

Millington, R.J., and J.M. Quirk. 1961. Permeability of porous solids. Trans. Faraday Soc. 57:1200–1207. doi:10.1039/tf9615701200

Moldrup, P., T. Olesen, J. Gamst, P. Schjønning, T. Yamaguchi, and D.E. Rolston. 2000. Predicting the gas diffusion coefficient in repacked soil: Water-induced linear reduction model. Soil Sci. Soc. Am. J. 64:1588–1594. doi:10.2136/sssaj2000.6451588x

Moldrup, P., T. Olesen, D.E. Rolston, and T. Yamaguchi. 1997. Modeling diffusion and reaction in soils: VII. Predicting gas and ion diffusivity in undisturbed and sieved soils. Soil Sci. 162:632–640. doi:10.1097/00010694-199709000-00004

Moldrup, P., T. Olesen, T. Yamaguchi, P. Schjønning, and D.E. Rolston. 1999. Modeling diffusion and reaction in soil: IX. The Buckingham–Burdine–Campbell equation for gas diffusivity in undisturbed soil. Soil Sci. 164:542–551. doi:10.1097/00010694-199908000-00002

Nakadai, T., M. Yokozawa, H. Ikeda, and H. Koizumi. 2002. Diurnal changes of carbon dioxide flux from bare soil in agricultural field in Japan. Appl. Soil Ecol. 19:161–171. doi:10.1016/S0929-1393(01)00180-9

Penman, H.L. 1940. Gas and vapour movement in the soil: I. The diffusion of vapours through porous solids. J. Agric. Sci. 30:437–462. doi:10.1017/S0021859600048164

Pingintha, N., M.Y. Leclerc, J.P. Beasley, G. Zhang, and C. Senthong. 2010. Assessment of the soil CO_2 gradient method for soil CO_2 efflux measurements: Comparison of six models in the calculation of the relative gas diffusion coefficient. Tellus 62:47–58. doi:10.1111/j.1600-0889.2009.00445.x

Pumpanen, J., H. Ilvesniemi, L. Kulmala, E. Siivola, H. Laakso, P. Kolari, et al. 2008. Respiration in boreal forest soil as determined from carbon dioxide concentration profile. Soil Sci. Soc. Am. J. 72:1187–1196. doi:10.2136/sssaj2007.0199

Risk, D., L. Kellman, and H. Beltrami. 2002. Soil CO_2 production and surface flux at four climate observatories in eastern Canada. Global Biogeochem. Cycles 16(4):1122. doi:10.1029/2001GB001831

Sanderman, J., and R. Amundson. 2010. Soil carbon dioxide production and climatic sensitivity in contrasting California ecosystems. Soil Sci. Soc. Am. J. 74:1356–1366. doi:10.2136/sssaj2009.0290

Sullivan, B.W., S. Dore, T.E. Kolb, S.C. Hart, and M.C. Montes-Helu. 2010. Evaluation of methods for estimating soil carbon dioxide efflux across a gradient of forest disturbance. Global Change Biol. 16:2449–2460.

Tang, J., D.D. Baldocchi, Y. Qi, and L. Xu. 2003. Assessing soil CO_2 efflux using continuous measurements of CO_2 profiles in soils with small solid-state sensors. Agric. For. Meteorol. 118:207–220. doi:10.1016/S0168-1923(03)00112-6

Tang, J., L. Misson, A. Gershenson, W. Cheng, and A.H. Goldstein. 2005. Continuous measurements of soil respiration with and without roots in a ponderosa pine plantation in the Sierra Nevada Mountains. Agric. For. Meteorol. 132:212–227. doi:10.1016/j.agrformet.2005.07.011

Turcu, V.E., S.B. Jones, and D. Or. 2005. Continuous soil carbon dioxide and oxygen measurements and estimation of gradient-based gaseous flux. Vadose Zone J. 4:1161–1169. doi:10.2136/vzj2004.0164

Verma, A.K., and T.J. Kelleners. 2012. Depthwise carbon dioxide production and transport in a rangeland soil. Soil Sci. Soc. Am. J. 76:821–828. doi:10.2136/sssaj2011.0416

Xiao, X., R. Horton, T.J. Sauer, J.L. Heitman, and T. Ren. 2014. Sensible heat balance measurements of soil water evaporation beneath a maize canopy. Soil Sci. Soc. Am. J. 78:361–368. doi:10.2136/sssaj2013.08.0371